Supplementary Information (SI) for CrystEngComm.
This journal is © The Royal Society of Chemistry 2024

Supporting Information

for

Complexes of N-Chloroquinuclidinium with Chloride: Strong Halogen Bonding via Chlorine Atoms

Maison Hardin,[a] Matthias Zeller[b] and Sergiy V. Rosokha*[a]

[a] Chemistry Department, Ball State University, Muncie, IN, 47304, USA
[b] Chemistry Department, Purdue University, West Lafayette, IN, 47907, USA
**Corresponding author, e-mail:svrosokha@bsu.edu.*

Details of the X-ray structural measurements.

The X-ray measurements were carried out on a Bruker AXS D8 Quest diffractometer. A Mo Kα radiation X-ray tube (λ = 0.71073 Å) was used for measurements of crystals **1** and Cu Kα radiation X-ray tube (λ = 1.54178 Å) was used for the measurements of crystals **2** and **3**. Reflections were indexed and processed, and the files were scaled and corrected for absorption using APEX4 or 5.[1] The space groups were assigned using XPREP within the SHELXTL suite of programs, the structures were solved by dual methods using ShelXT and refined by full-matrix least-squares against F^2 with all reflections using Shelxl2019 with the graphical interface Shelxle.[2-4] Complete crystallographic data, in CIF format, have been deposited with the Cambridge Crystallographic Data Centre. CCDC 2384417-2384419 contain the supplementary crystallographic data for this paper. These data can be obtained free of charge via www.ccdc.cam.ac.uk/data_request/cif .

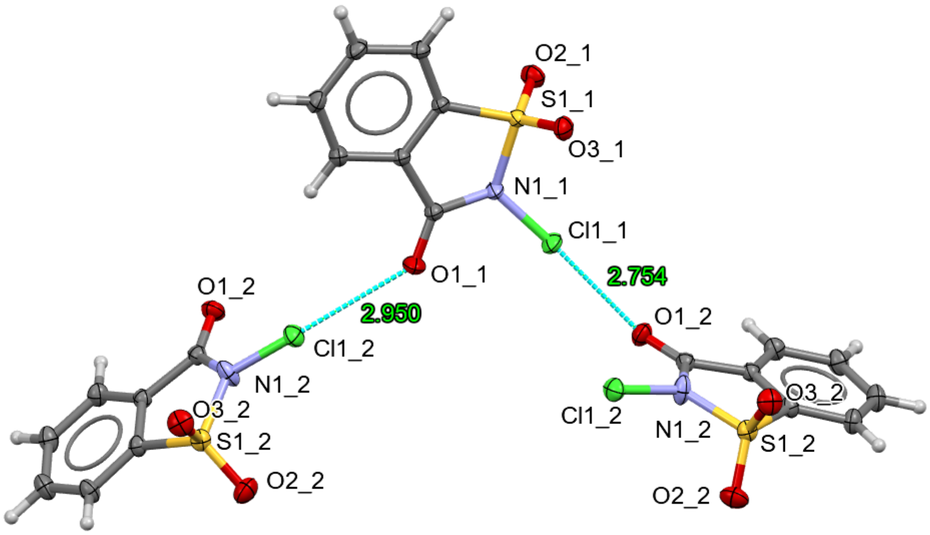

Figure S1. X-ray structure of **1** showing two non-equivalent Cl…O halogen bonds.

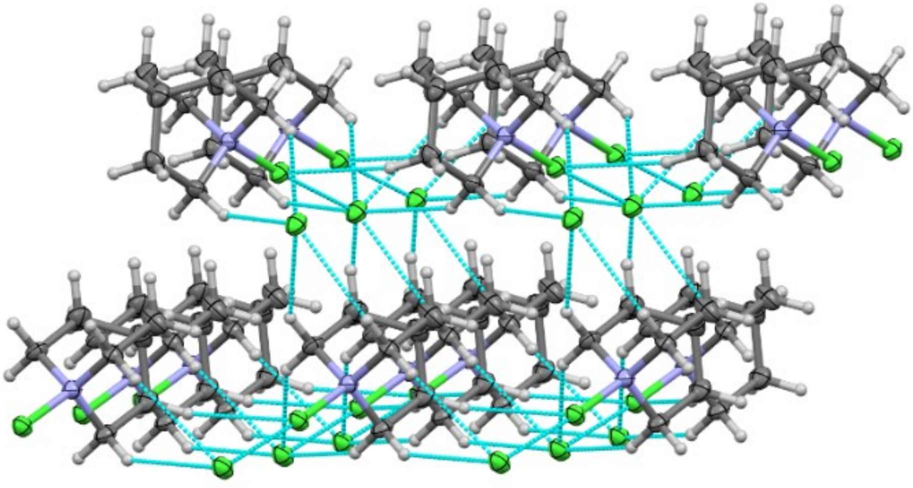

Figure S2. X-ray structure of **2**. Blue lines show short contacts between ClQN$^+$ and Cl$^-$

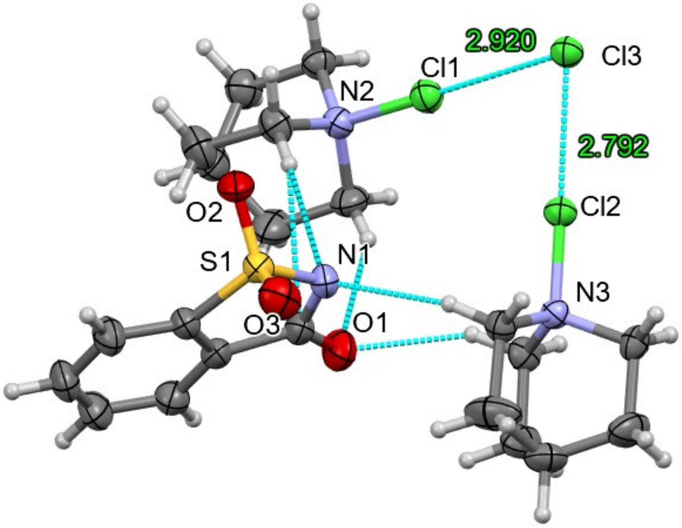

Figure S3. X-ray structure of **3** showing two non-equivalent Cl…Cl$^-$ halogen bonds.

Computational details.

Geometries of the complexes were optimized without constraints via M06-2X/def2-TZVPP calculations (with ultrafinegrid option) using the Gaussian 09 suite of programs.[5-7] The absence of imaginary frequencies confirmed that the optimized structures represent true minima. Calculations were done with acetonitrile as the medium using a polarizable continuum model.[8] An earlier analysis demonstrated that intermolecular associations are well-modelled using this method.[9,10] The def2-TZVPP basis set does not include a diffuse function since previous analysis demonstrated that very similar results were obtained in the modelling of noncovalent interactions involving anions with the triple-ζ basis sets with and without diffuse functions.[11] Binding energies, ΔE were determined as the difference between the sums of the electronic energy and zero-point energy (ZPE) of the optimized complex and its components. The energies of the optimized complexes and their components are listed in Table S1. QTAIM[12] and NCI[13] analyses of the solid-state associations and optimized complexes were performed using the atomic coordinates extracted from the X-ray structures with Multiwfn and visualized using VMD programs.[14, 15] (The NCI setting was: isovalue = 0.5, color-coded with sgn(λ2)ρ in the range from −0.04 a.u. (blue, strong attractive interaction) to 0.02 a.u. (red, strong nonbonded overlap). Characteristics of the BCPs obtained from QTAIM analysis are listed in Table S2. Energy decomposition analyses (EDA) were carried out using the Amsterdam density functional (ADF) of the Amsterdam Modelling Suite[16,17] via single-point calculations with the B3LYP-D3 functional (since it allowed evaluation of the dispersion component of the interaction energy) and the TZ2P basis set available in AMS. The results of EDA are listed in Table S3. QTAIM and EDA were performed using atomic coordinates of the associations extracted from the X-ray structures (which are shown in Figure 4 in the text).

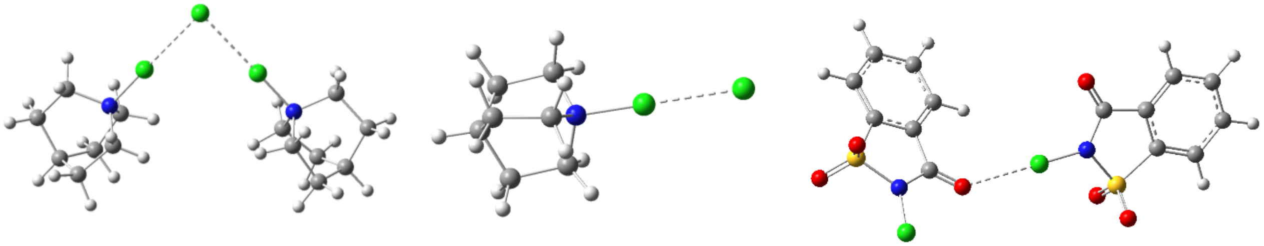

Figure S4. Optimized structures of the 2:1 and 1:1 complexes of $ClQN^+$ and Cl^- and of the HaB dimer of ClSac.

Table S1. Characteristics of the optimized HaB complexes and their components

Complex	E, Hartree	ZPE, Hartree	$d_{N\text{-}Cl}$, Å	$d_{Cl\ldots X}$, Å	ΔE, kcal/mol
$ClQN^+$-Cl^-	-1249.67537	0.20134	1.801	2.641	-8.9
$(ClQN^+)_2$-Cl^-	-2038.97684	0.40345	1.769	2.793	-7.9[a]
$ClQN^+$	-789.29087	0.20127	1.736		
Cl^-	-460.37029				
ClSac	-1407.92152	0.107484			

a) Per one bond

Table S2. Characteristics of the bond critical points (in a.u.) [a]

Complex	Contact	#[b]	$d_{Cl..X}$,Å	$\rho(\mathbf{r})$	$G(\mathbf{r})$	$V(\mathbf{r})$	$H(\mathbf{r})$	$\nabla^2\rho(\mathbf{r})$	ELF	MBO
ClQN$^+$-Cl$^-$	N-Cl	-	1.804	0.181	0.0894	-0.1958	-0.106	-0.068	0.776	1.00
	Cl…Cl	1	2.664	0.037	0.0259	-0.0274	-0.0015	0.098	0.169	0.19
	H…Cl	2	2.868	0.008	0.0050	-0.0039	0.0011	0.024	0.030	<0.05
	H…Cl	3	2.765	0.009	0.0061	-0.0048	0.0013	0.030	0.035	<0.05
	H…Cl	4	2.747	0.010	0.0063	-0.0050	0.0013	0.031	0.036	<0.05
	H…Cl	5	2.765	0.009	0.0061	-0.0048	0.0013	0.030	0.035	<0.05
	H…Cl	6	2.747	0.010	0.0063	-0.0050	0.0013	0.031	0.036	<0.05
	H…Cl	7	2.868	0.009	0.0061	-0.0048	0.0013	0.030	0.035	<0.05
(ClQN$^+$)$_2$-Cl$^-$	N-Cl	-	1.786	0.191	0.0897	-0.2079	-0.118	-0.114	0.805	1.05
	Cl…Cl	1	2.791	0.027	0.0205	-0.0197	0.0008	0.085	0.108	0.12
	Cl…Cl	2	2.920	0.021	0.0157	-0.0141	0.0016	0.069	0.079	0.10
	H…Cl	3	2.867	0.008	0.0048	-0.0038	0.0011	0.024	0.029	<0.05
	H…Cl	4	2.784	0.009	0.0058	-0.0045	0.0012	0.028	0.033	<0.05
	H…Cl	5	2.619	0.012	0.0083	-0.0068	0.0015	0.039	0.044	<0.05
	H…Cl	6	2.847	0.008	0.0051	-0.0040	0.0011	0.025	0.030	<0.05
	H…Cl	7	2.573	0.013	0.0091	-0.0075	0.0016	0.043	0.047	<0.05
(ClSac)$_2$	N-Cl	-	-	0.010	0.0090	-0.0066	0.002	0.046	0.019	0.99
	Cl-O	-	2.753	0.228	0.1179	-0.3033	-0.185	-0.270	0.811	<0.05

a) Calculated using coordinates of the clusters (see below) extracted from the solid-state (X-ray) structures. b) See the figure below.

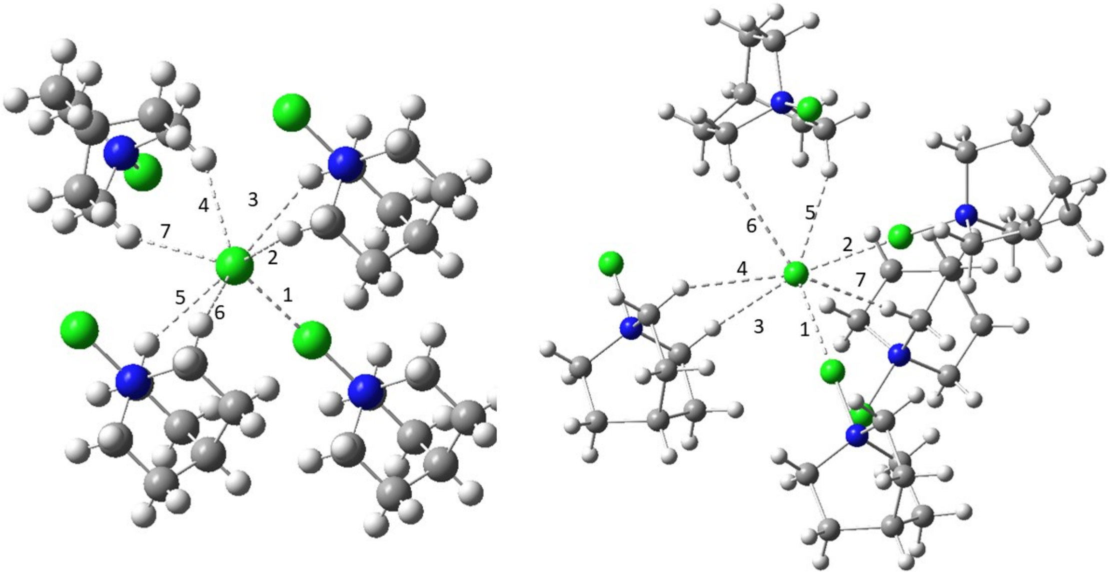

Table S3. Interaction energies and their components (in kcal/mol) from the EDA analysis.

Complex	ΔE_{Pauli}	ΔE_{es}	ΔE_{oi}	ΔE_{disp}	E_{int}
ClQN$^+$-Cl$^-$	33.83	-85.89	-44.82	-1.61	-98.49
(ClQN$^+$)$_2$-Cl$^-$	38.35	-147.35	-54.52	-2.95	-166.47
(ClSIM)$_2$-Cl$^-$	31.91	-21.31	-34.47	-2.71	-26.59
(ClSac)$_2$	5.56	-4.48	-2.19	-2.25	-3.36

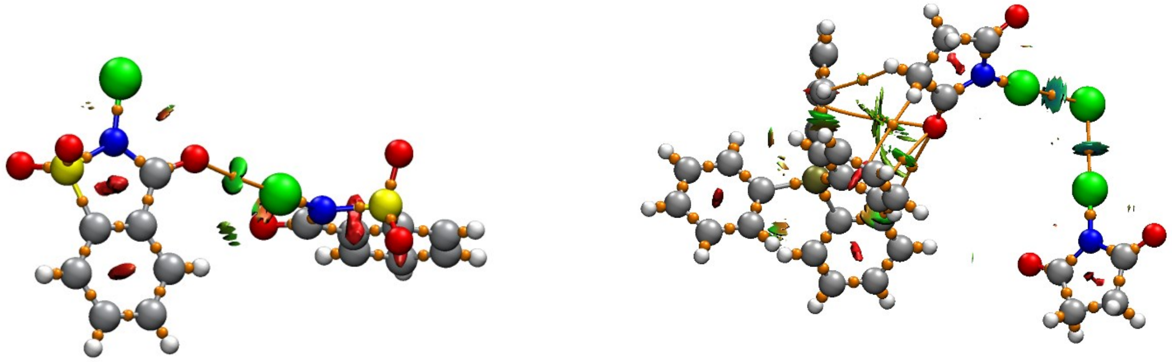

Figure S5. QTAIM and NCI analyses of the HaB complexes in **1** (which is characterized by a longer HaB of 2.950 Å (left), and in complex (CLSIM)$_2$Cl (coordinates are extracted from the structure CCDC refcode WEZVUS). The bond paths and critical (3, -1) points (QTAIM) are shown as orange lines and spheres, and blue-green areas (NCI) indicate bonding interactions.

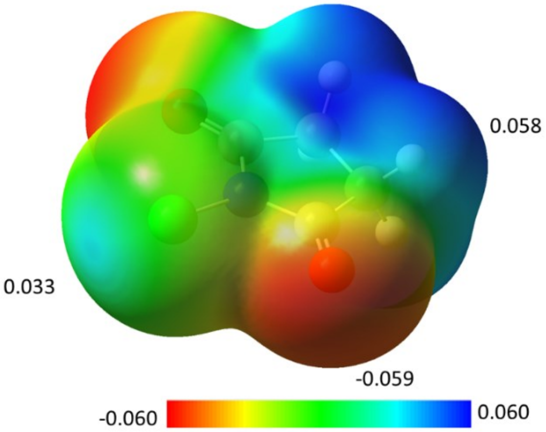

Figure S6. Surface electrostatic potentials (at 0.001 a.u. electron density) of ClSim.

References.

1 *Bruker Apex3 v2016.9-0, SAINT V8.37A,* Bruker AXS Inc.: Madison, WI, 2016.

2 (a) Sheldrick, G. *SHELXTL suite of programs,* Version 6.14, 2000-2003, Bruker AXS Inc.: Madison, WI, 2003. (b) G. M. Sheldrick, Acta Cryst. A64, 2008, 112.

3 G.M. Sheldrick, *Acta Cryst*. A71 2015, 3.

4 C. Hübschle, G. Sheldrick and B. Dittrich, *J. Appl. Crystallogr.,* 2011, **44**, 1281.

5 Gaussian 09, Revision C.01, M. J. Frisch, G. W. Trucks, H. B. Schlegel, G. E. Scuseria, M. A. Robb, J. R. Cheeseman, G. Scalmani, V. Barone, B. Mennucci, G. A. Petersson, H. Nakatsuji, M. Caricato, X. Li, H. P. Hratchian, A. F. Izmaylov, J. Bloino, G. Zheng, J. L. Sonnenberg, M. Hada, M. Ehara, K. Toyota, R. Fukuda, J. Hasegawa, M. Ishida, T. Nakajima, Y. Honda, O. Kitao, H. Nakai, T. Vreven, J. A. Montgomery, Jr., J. E. Peralta, F. Ogliaro, M. Bearpark, J. J. Heyd, E. Brothers, K. N. Kudin, V. N. Staroverov, R. Kobayashi, J. Normand, K. Raghavachari, A. Rendell, J. C. Burant, S. S. Iyengar, J. Tomasi, M. Cossi, N. Rega, J. M. Millam, M. Klene, J. E. Knox, J. B. Cross, V. Bakken, C. Adamo, J. Jaramillo, R. Gomperts, R. E. Stratmann, O. Yazyev, A. J. Austin, R. Cammi, C. Pomelli, J. W. Ochterski, R. L. Martin, K. Morokuma, V. G. Zakrzewski, G. A. Voth, P. Salvador, J. J. Dannenberg, S. Dapprich, A. D. Daniels, O. Farkas, J. B. Foresman, J. V. Ortiz, J. Cioslowski and D. J. Fox, Gaussian, Inc., Wallingford CT, 2009.

6 Y. Zhao and D. G. Truhlar, *Theor. Chem. Acc.*, 2008**, 120,** 215-41.

7 F. Weigend and R. Ahlrichs, *Phys. Chem. Chem. Phys*., 2005**, 7**, 3297.

8 J. Tomasi, B. Mennucci and R. Cammi, *Chem. Rev.*, 2005, **105**, 2999−3093.

9 Z. Zhu, Z. Xu and W. Zhu, *J. Chem. Inf. Model*., 2020, **60**, 2683.

10 K. Wang, J. Lv and J. Miao, *Theor. Chem. Acc.,* 2015, **134**, 5.

11 A. Bauzá, D. Quiñonero, P. M. Deyà and A. Frontera, *J. Phys. Chem. A,* 2013, **117**, 2651.

12 R. F. W. Bader, *Chem. Rev.,* 1991, **91**, 893.

13 E. R. Johnson, S. Keinan, P. Mori-Sánchez, J. Contreras-García, A. J. Cohen and W. Yang, *J. Am. Chem. Soc.*, 2010, **132**, 6498.

14 T. Lu and F. Chen, *J. Comput. Chem.*, 2012, **33**, 580.

15 W. Humphrey, A. Dalke and K. Schulten, *J. Mol. Graphics*, 1996, **14**, 33.

16 E. J. Baerends, T. Ziegler, J. Autschbach, D. Bashford, A. Berger, A. Bérces, F. M. Bickelhaupt, C. Bo, P. L. de Boeij, P. M. Boerrigter and S. Borini, et.al. ADF2012.01; SCM: Amsterdam, 2012.

17 (a) F. M. Bickelhaupt and E. J. Baerends,. Kohn-Sham density functional theory: predicting and understanding chemistry. In *Reviews in Computational Chemistry*; John Wiley & Sons, Ltd, 2000; 1. (b) G. te Velde, F. M. Bickelhaupt, E. Baerends, C. Fonseca Guerra, S. J. A. van Gisbergen, J. G.; Snijders and T. Ziegler, *J. Comput. Chem.,* 2001, **22**, 931.